Heliyon 11 (2025) e41009

Contents lists available at ScienceDirect

Heliyon

journal homepage: www.cell.com/heliyon

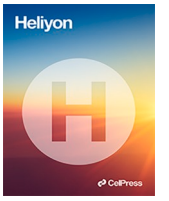

Research article

Differences of simulated ankle dorsiflexion limitation on lower extremity biomechanics during long jump takeoff

Zanni Zhang [a], Datao Xu [a,b], Xiangli Gao [a], Huiyu Zhou [a], Julien S. Baker [a,c], Zsolt Radak [a,d], Yaodong Gu [a,*]

[a] Faculty of Sport Science, Ningbo University, Ningbo, 315211, China
[b] Faculty of Engineering, University of Pannonia, Veszprem, 8201, Hungary
[c] Centre for Population Health and Medical Informatics, Hong Kong Baptist University, Kowloon, China
[d] Research Institute of Sport Science, University of Physical Education, Budapest, 1123, Hungary

ARTICLE INFO

Keywords:
Ankle
Range of motion
Lower extremity
Biomechanics
Jumping

ABSTRACT

The long jump is an athletic event that demands speed, power, force application, and balance, with each phase being critical to overall performance. However, previous research has neglected the limiting effect of the wedge pedals on ankle dorsiflexion range of motion. This cross-sectional study investigated biomechanical changes in the lower extremities during long jumps under varying degrees of ankle dorsiflexion. Thirty male Division II long jump athletes executed jumps under three conditions: no dorsiflexion, with 10° dorsiflexion restriction, and with 20° dorsiflexion restriction. A Vicon motion capture system with eight cameras and an AMTI force platform were used to collect biomechanical data simultaneously during the long jump. The angles, moments, and velocities of the ankle, hip, and knee joints during takeoff were simulated and calculated using a musculoskeletal model. Between-group variations were assessed using one-way repeated measures ANOVA, with statistical parametric mapping (SPM1D) applied for analysis. Results showed that as ankle restriction increased, vertical velocity gain increased: NW (3.34 ± 0.21 m/s), 10W (3.65 ± 0.14 m/s), and 20W (3.77 ± 0.12 m/s) ($p < 0.001$). Horizontal velocity loss was significantly higher only at 20W ($p = 0.002$). Peak extension angle, angular velocity, and power were highest at 10W for the knee and hip joints ($p < 0.05$). Joint forces at the ankle, knee, and hip were significantly affected by different pedal angles ($p < 0.001$). Athletes with a 10° ankle dorsiflexion limit showed increased vertical velocity with minimal horizontal velocity loss, potentially enhancing performance. This limit also increased muscle co-activation around the knee, possibly stabilizing it. Athletes should consider a 10° ankle dorsiflexion limit in training to improve performance and reduce injury risk.

1. Introduction

The long jump is a track and field event where athletes utilize a combination of speed, strength, power, and balance to achieve maximal horizontal displacement [1,2]. It is divided into four distinct phases: the approach phase, the takeoff phase, the flight phase, and the landing phase, each of which is integral to overall performance. The approach phase involves building up speed while

* Corresponding author.
E-mail address: guyaodong@nbu.edu.cn (Y. Gu).

https://doi.org/10.1016/j.heliyon.2024.e41009
Received 1 August 2024; Received in revised form 4 December 2024; Accepted 4 December 2024
Available online 13 December 2024

maintaining control and proper posture, and the takeoff phase converts this horizontal speed into vertical lift [3]. During the flight phase, the athlete must maintain balance and prepare for a controlled landing, while the landing phase focuses on minimizing distance loss and injury risk. Throughout history, notable achievements, such as Mike Powell's record-breaking long jump in 1991 [4], have shown the evolution of techniques and training methods in the sport. In modern athletics, maximizing performance in each of these phases has been a primary goal in long jump training.

In training, the takeoff board is widely used to improve the takeoff technique by adjusting the takeoff angle, thereby enhancing performance [4,5]. The takeoff phase is pivotal as it sets the trajectory and velocity for the subsequent phases. While tools like the takeoff board have proven effective in refining technique, pedals—which restrict ankle dorsiflexion—are increasingly used to further optimize the takeoff phase [6]. However, the impact of dorsiflexion restriction on overall performance and injury risk remains underexplored. Limited ankle dorsiflexion affects power output and postural control, both of which are critical in high-speed, high-impact sports like the long jump [7]. Research has demonstrated that augmenting the initial contact angle and range of motion of the ankle joint in one leg can enhance energy efficiency in the lower limb joints, diminish peak forces on the anterior cruciate ligament (ACL), and decrease impact loads on the lower limb joints. This, in turn, reduces the risk of lower limb injuries, including ACL injuries [8,9]. Conversely, limited ankle mobility can significantly impair biomechanical performance and elevate the risk of injury [10–12]. For instance, healthy female athletes generally exhibit a greater dynamic functional range of motion (DFROM) during jump landing. A reduced DFROM has been correlated with an elevated risk of injury during these landings [12]. Similarly, limited ankle mobility has been shown to increase the risk of injury during jumping [13,14]. Overall stability limit scores were significantly lower with ankle immobilization, as ankle restriction interferes with anatomical dominance and muscle activation at the ankle joint [15]. A previous study using the Adaptive Neuro-Fuzzy Inference System (ANFIS) to estimate ankle angles in a healthy population confirmed that kinematic variations of the ankle in the sagittal, coronal, and horizontal planes may contribute to osteoarthritis of the knee [16, 17]. These findings underscore the importance of ankle flexibility and strength in optimizing long jump performance and minimizing injury risks. Existing research, however, lacks a comprehensive investigation into how different degrees of dorsiflexion restriction affect biomechanical performance during long jump takeoff. While studies on general ankle mobility exist, few focus on its application to the long jump, particularly concerning specific restriction angles.

In the long jump, the velocity at takeoff is crucial, encompassing both vertical and horizontal components [18]. During the long jump, the angle of the pedal significantly affects the athletes' jumping posture and the biomechanical properties of the lower limbs. The maximal increase in vertical velocity from the moment of touchdown to the jump is associated with a low center of gravity, a greater knee extension angle at touchdown, and a low peak knee flexion velocity, which is related to the ability to resist knee flexion [19–21]. The combination of these three variables explains the change in vertical velocity gain from touchdown to jump. Similarly, greater horizontal velocity loss during the jump phase is associated with increased height change, greater hip adduction, and more pronounced hip extension [19–21]. The combination of these three variables explains the horizontal velocity change from touchdown to jump, but the optimal ankle dorsiflexion restriction angles for balancing performance gains with injury prevention remain unclear. Therefore, understanding the interaction between ankle dorsiflexion restriction angles and these biomechanical variables is crucial for optimizing jump performance.

Given the widespread use of wedge pedals in training, it is essential to determine the optimal degree of dorsiflexion restriction that maximizes takeoff performance while minimizing the risk of injury. Without proper knowledge, athletes and coaches may inadvertently over-restrict or under-restrict dorsiflexion, leading to either suboptimal performance or an increased risk of musculoskeletal injuries, particularly in the ankle, knee, and hip joints. A systematic examination of the biomechanical effects of varying degrees of restriction could fill this gap and provide critical insights for safe and effective training practices. Therefore, the purpose of this study is to investigate the effects of different ankle dorsiflexion restriction angles (0°, 10°, and 20°) on the biomechanics of the lower limb during long jump takeoff. By assessing the vertical and horizontal velocities, joint angles, and muscle activation patterns, this study aims to provide a more scientific theoretical basis for training long jumpers. The findings will offer practical guidance for coaches and athletes, helping them tailor training programs that not only enhance performance but also minimize injury risk.

2. Methods Details

2.1. Study design

This study utilized a cross-sectional design to explore the biomechanical effects of varying degrees of ankle dorsiflexion restriction during long jump takeoff. Thirty male Division II long jump athletes participated in the study. Each athlete completed long jumps under three different dorsiflexion conditions: no wedge (NW), 10° dorsiflexion restriction (10W), and 20° dorsiflexion restriction (20W). The Vicon motion capture system with eight cameras and an AMTI force platform was used to simultaneously collect biomechanical data, including joint angles, moments, and velocities at the ankle, knee, and hip during the takeoff phase. Electromyography (EMG, Delsys, Boston, MA, USA) was also used to measure muscle activation patterns. Data from the jumps were processed and analyzed using one-way repeated measures ANOVA and statistical parametric mapping (SPM1D) to examine the differences between the three dorsiflexion conditions.

2.2. Study Participant Details

In this study, a priori power analysis was conducted using G*Power (version: 3.1.9.7; Henri Düsseldorf University, Düsseldorf, Germany) software to determine the sample size necessary for the experimental design [22]. With the statistical power and

significance level fixed at 0.80 and 0.05 [24], the number of repeated measurements was calculated to be 6 using 3 groups. The results showed that a sample size of at least 30 participants was required to achieve a medium effect size of 0.25. A total of 30 male long jumpers were recruited from Ningbo University, with a mean age of 21.45 ± 3.14 years, a mean height of 179.30 ± 3.80 cm, and a mean weight of 72.20 ± 5.05 kg. The inclusion criteria for participants were as follows: (1) Participants were level II long jumpers and members of the track and field team at Ningbo University (the standard for level II long jumpers is a long jump of 6.7 m and above). (2) Participants with a history of lower limb injuries in the last six months that could impact performance, or the study results were excluded. (3) Participants who had undergone any lower extremity surgery were excluded due to potential biomechanical alterations that could affect the results. (4) Participant with chronic diseases or conditions (e.g., cardiovascular, musculoskeletal, or neurological disorders) that might interfere with performance or affect the study's outcome was excluded. (5) Participants who did not consistently meet the long jump training of three times per week for at least 2 h per session were excluded from the study. (6) Participants with a history of recurrent ankle sprains or chronic ankle instability, even if the most recent injury was more than six months prior, were excluded to ensure accurate biomechanical assessment. (7) Participants currently using medication that could affect their muscle function, balance, or neuromuscular performance, such as painkillers, muscle relaxants, or anti-inflammatory drugs, were excluded. (8) Participants who could not fully comply with the experimental procedures, including warming up, following takeoff instructions, or adhering to the reflective marker placement protocol, were excluded. (9) Participants who did not agree to wear the standardized footwear provided for the experiment, or whose foot structure required specialized footwear (e.g., orthotics) that might influence the outcomes, were excluded. (10) Participants showing signs of excessive fatigue or overtraining syndrome on the day of testing, which

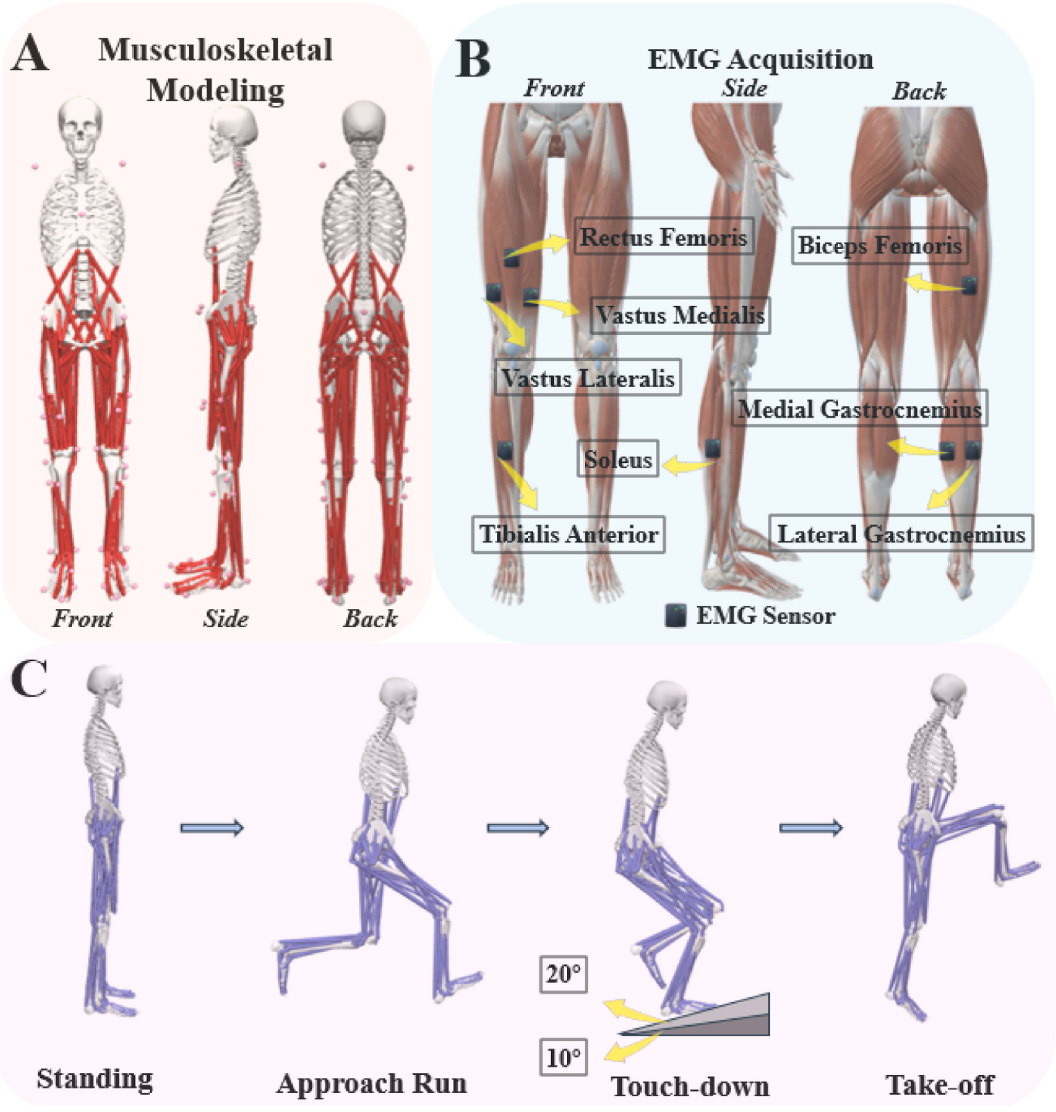

Fig. 1. **(A)** Illustration of the schematic representation of reflective marker placement on body skeletal landmarks. **(B)** Illustration of the placement of an EMG electrode on the lower limb of a human. **(C)** Illustration of the long jump biomechanical test process.

could compromise performance or produce unreliable data, were excluded. (11) Participants with pre-existing biomechanical abnormalities (e.g., leg length discrepancies, flat feet, or high arches) that could interfere with the takeoff phase mechanics were excluded from the study. (12) All participants provided written informed consent before data collection and ethical approval for the study was obtained from the University of Ningbo ethical committee (Protocol Code: RAGH20240501).

2.3. Data collection procedures

All tests were conducted in the Exercise Biomechanics Laboratory at the Institute of Greater Health, Ningbo University. A Vicon motion capture system (Oxford Metrics Ltd, Oxford, UK), equipped with 8 cameras, was used to capture the motion data of the participants during the long jump task. The sampling frequency was set at 200 Hz [23]. The Vicon motion capture system used in this study was carefully calibrated before each testing session to ensure precise measurement of joint kinematics and movements. Calibration involved positioning reflective markers in known positions within the capture volume and adjusting the system to optimize camera alignment and accuracy. This process was repeated at the start of each data collection session to maintain measurement precision. The sampling frequency of the force platform (AMTI, Watertown, MA, USA) was set to 1000 Hz to collect motion data during the long jump. The two experimental setups were synchronized. The initial contact point was identified when the vertical ground reaction force exceeded 10 Nm [24]. The **AMTI force platform** was calibrated according to the manufacturer's guidelines before each testing session to ensure accurate recording of ground reaction forces (GRFs). This calibration process involved applying known loads to the platform and adjusting the system to ensure correct force output readings. All participants wore tight shorts and shirts. Consistent with previous studies, each participant was affixed with 38 spherical reflective markers with a diameter of 12.5 mm to identify movement patterns during each trial [25]. Reflex markers were placed at specific anatomical landmarks on the body as shown in Fig. 1A, The SENIAM guidelines [26] were followed for the placement of the EMG sensors. Eight EMG sensors were mounted on the muscle bodies of the soleus, medial and lateral gastrocnemius, tibialis anterior, rectus femoris, extensor fasciae latae, intenser fasciae latae, and biceps femoris muscles shown in Fig. 1B. The EMG system used to capture muscle activation data was also calibrated following standardized procedures. This involved testing the EMG sensors for signal accuracy and adjusting the system to ensure noise reduction and consistent signal capture. Skin preparation procedures (e.g., shaving, and cleaning gel) were implemented to enhance the quality of the signals. The EMG system has been validated in prior research, demonstrating its reliability in recording muscle activation during sports movements. The Vicon system, AMTI force platform, and EMG system are synchronized for data acquisition.

Participants warmed up for 15 min at a pace of their choice on the athletic field wearing a tight-fitting shirt and shoes that met the requirements for the official experiment, participants then practiced long jump-specific preparatory activities to ensure that each participant was able to perform to his or her maximum potential in the experiment. Each participant was given three opportunities to familiarize themselves with the test movements. Following the warm-up phase, subjects underwent thorough familiarization with the experimental conditions and procedures before proceeding with the full test protocol. Prior to formal data collection, subjects stood on a force plate to record static coordinates. Each subject positioned their feet parallel to the y-axis, extended their arms 45° from the sides of the body, and maintained forward gaze until the completion of static data collection.

To collect biomechanical data and to ensure that the athletes were able to accurately step onto the springboard, the athletes first performed a counter-run to determine the starting point of the eight-step run, and after determining the starting point, on command, they immediately performed a complete long jump test consisting of the eight-step run, jump, lift, and landing [27], limitation of ankle dorsiflexion with no wedge (NW), 10° wedge (10W) and 20° wedge (20W), respectively. Fig. 1C illustrates a complete long jump takeoff. Participants were asked to perform to the maximum potential possible [28–30]. The data collected specifically pertained to the participant's initial leg, defined as the leg that first contacted the springboard [25]. During the long jump task, a failure was recorded if any participant was observed not stepping onto the springboard when or if they did not complete the movement in its entirety. Six successful datasets were collected using the dominant leg, which equates to 18 datasets per participant at three different starting angles. A 2-min rest period between each test and a 5-min rest period between jumps at each takeoff angle was used to prevent participants from over-fatiguing.

2.4. Musculoskeletal modeling and data processing programs

The kinematics and kinetics data collected from Vicon were exported to C3D file format and then converted to a coordinate system, low pass filtered, data extraction, and formatted for kinematic and kinetic data using MATLAB (MathWorks, Massachusetts, USA). The C3D files were converted to trc file format and mot file format using MATLAB and imported into OpenSim (Stanford University, Stanford, CA, USA) to calculate biomechanical parameters [31]. A musculoskeletal model comprising 23 degrees of freedom and 92 muscle actuators was employed for all musculoskeletal simulations [32]. The Scale Tool in OpenSim allows researchers to create subject-specific musculoskeletal models by adjusting a generic model to match the body dimensions of individual participants [32]. It uses anthropometric data (e.g., height, limb lengths) and marker positions from the motion capture data to scale the generic model so that it accurately reflects each participant's musculoskeletal structure. Specifically, scaling factors for individual body segments were determined by comparing distances between two markers on the segment, measured during a static standing trial, with corresponding distances on the generic model. These factors were then used to adjust segment lengths, inertial properties, muscle attachment points, and other parameters accordingly.

The accuracy of the model was improved by using specific equations and plug-ins from OpenSim to calculate the joint angle using the inverse kinematics algorithm, the joint moment using the inverse dynamics algorithm, and applying a residual reduction algorithm (RRA) to minimize dynamic inconsistencies in the model [35]. RRA also computes an adjusted location of the torso center of mass (COM)

to minimize residual moments in the frontal and transverse planes [35]. The inverse kinematics tool optimizes the calculation of joint angle by weighted least squares to minimize the differences between the model and experimental marker positions, joint moments for each degree of freedom of the model were computed using the inverse kinematics tool. Joint power was derived by multiplying angular velocity by the joint moment at each time point [36,37]. Static optimization algorithms were employed to compute muscle activation and muscle force. Joint forces were derived from the muscle force outputs of the static optimization process using the joint reaction force tool in OpenSim [38]. The Joint Reaction Force Tool calculates the forces acting on the joints based on the muscle forces derived from the Static Optimization process. It provides information on the compressive, shear, and rotational forces acting on the joints, which are essential for understanding joint loading and the potential for injury. Fig. 2 shows the workflow of the musculoskeletal modeling process used to calculate muscle force, muscle activation, COM, and joint force. Calculation of vertical velocity gain and horizontal velocity loss during the long jump start based on kinematic data. The regression equations for vertical velocity gain and horizontal velocity loss from the instant of touchdown to the instant of takeoff are [19]:

$$VY_{TD-TO} = -3.283 - 5.591\, H_{TD} + 0.0851\, A_{(KNEE)TD} - 0.188\, PAV_{(KNEE)} \quad (1)$$

H_{TD} represents the height of the center of mass at touchdown, $A_{(KNEE)TD}$ represents the knee joint angle at touch-down, $PAV_{(KNEE)}$ represents the peak knee flexion velocity.

$$VX_{TD-TO} = 0.370 + 4.40\, H_{TD-TO} + 0.041\, A_{(HIP-A)TD-MHA} - 0.008\, A_{(HIP-E)TD-TO} \quad (2)$$

$A_{(HIP-A)\ TD-MHA}$ represents the range of hip adduction from touch-down to its minimum hip adduction angle, $A_{(HIP-E)TD-TO}$ represents the range of hip joint extension throughout the takeoff phase, H_{TD-TO} represents the change in height during the takeoff phase.

Muscle activations computed using the static optimization algorithm were compared to surface EMG activity recorded experimentally to validate the model. Appropriate signal-to-noise ratios were determined by performing residual analysis on a subset of data

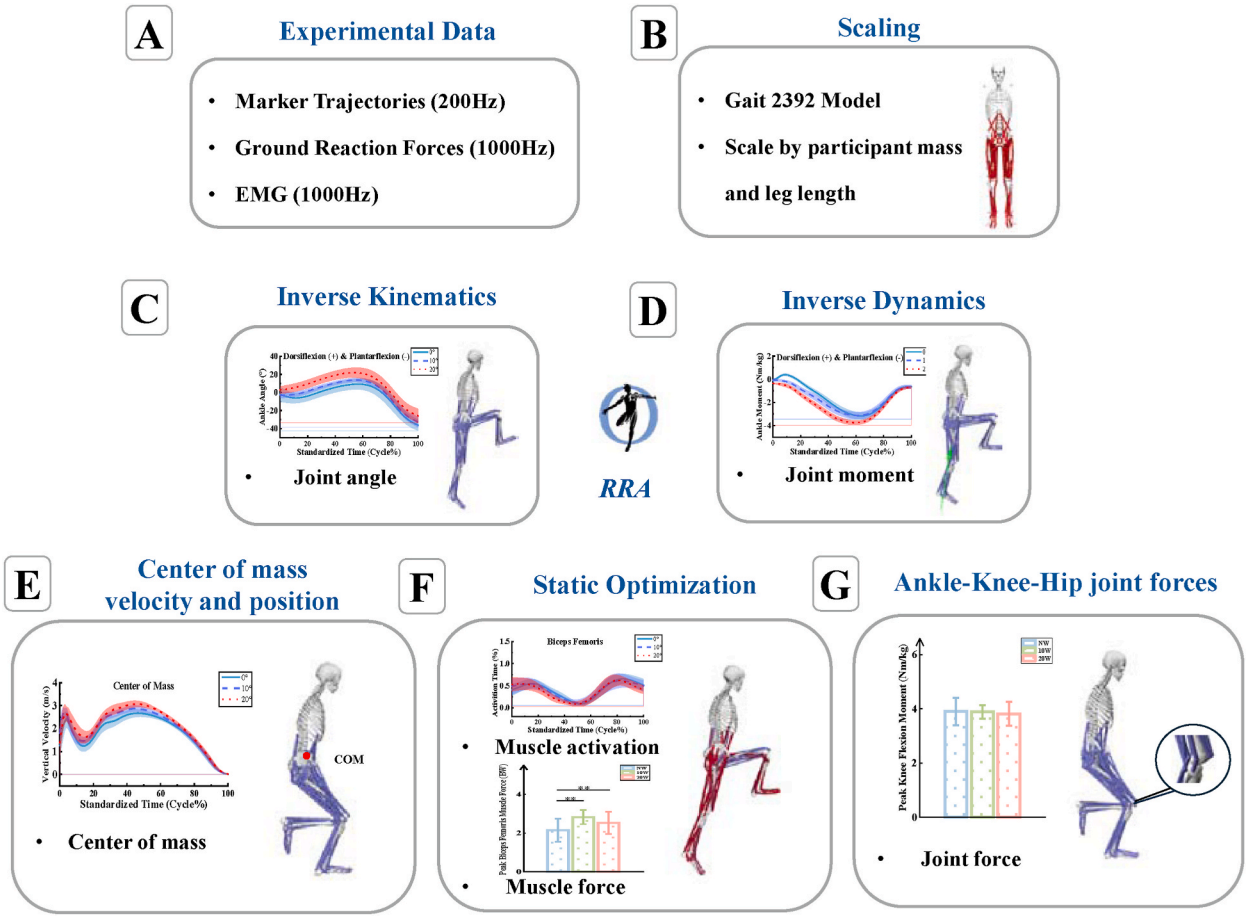

Fig. 2. Workflow of the musculoskeletal modeling process used to calculate muscle force, muscle activation, COM, and joint force. **(A)** Importing experimental data into Opensim software. **(B)** Scaling of model. **(C)** Inverse Kinematics. **(D)** Inverse Dynamics. **(E)** Center of mass. **(F)** Static Optimization. **(G)** Joint force. RRA: Residual Reduction Algorithm.

from previous studies. To compute co-activation for the descending phase of the long jump takeoff, the following equation was applied [33]:

$$Muscleco - activation(\%) = \left(\frac{RMSEMG_{antaonist}}{RMSEMG_{agonist}}\right)*100 \quad (3)$$

Surface EMG signals were initially filtered using a fourth-order Butterworth band-pass filter with a frequency range of 10–400 Hz. Subsequently, the signals underwent full-wave rectification and were further filtered with a low-pass filter at a cutoff frequency of 6 Hz [34]. In addition, the EMG signals were normalized by dividing the EMG amplitude by the maximum root-mean-square amplitude and further adjusted by MVC to derive the activation level of each muscle. The muscle activation data recorded by the EMG sensors were then compared with those obtained from the musculoskeletal model simulations to validate the reliability and precision of the model. Fig. 3 shows that no significant differences were found when comparing muscle activation in the EMG data and the musculoskeletal model.

2.5. Quantification and statistical analysis

Before conducting statistical analysis, normality testing was performed on all experimental data using the Shapiro-Wilk test. If the data did not satisfy the normality criteria, Kruskal-Walli's test was utilized to evaluate differences in kinematic and kinetic variables among different angles during the long jump. In the statistical parametric mapping (SPM) analysis, kinematic and kinetic data from the takeoff phase were extracted and processed using a custom MATLAB script. The data points were interpolated to generate a time series curve comprising 101 data points, representing the entire landing phase from 0 % to 100 % [35]. Subsequently, statistical analysis was

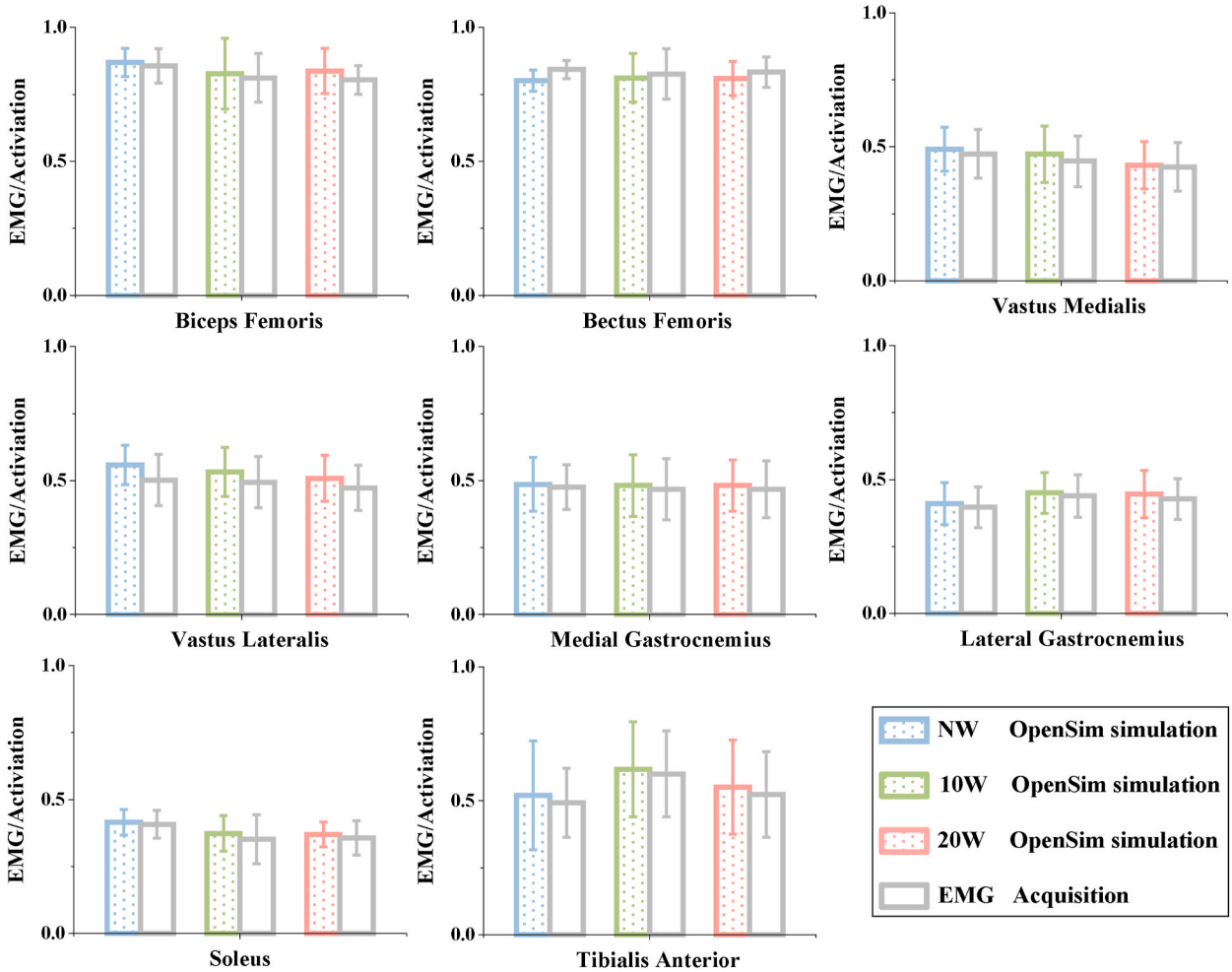

Fig. 3. EMG/Activation of the lower limb muscles. The results of the EMG acquisition were calculated from the collected surface EMG signal. The OpenSim simulation results were derived from the constructed musculoskeletal model. Muscle activation is normalized to 0–1, which represents no activation and full activation.

performed using one-dimensional parameter statistical mapping (SPM1D) scripts for one-factor repeated measures analysis of variance, with a significance threshold set at 0.05. For conventional discrete variable analysis, MATLAB scripts were employed to extract data from the long jump takeoff phase. All analyses of traditional discrete variables were conducted using SPSS 27.0 for Windows™ software, with statistical significance defined as $P < 0.05$. Finally, the obtained data were inputted into Origin 2022 software for visualization and plotting.

3. Results

3.1. Kinematics

For the results of the joint angle, as the ankle joint restriction angle increased, the ankle dorsiflexion angle increased in the 10 %–70 % phase ($p < 0.001$) and 90 %–100 % phase ($p = 0.017$). With a 20° restriction, it increased throughout the 0 %–100 % phase ($p < 0.001$); the hip extension angle increased in the 10 %–83 % phase ($p < 0.001$). Hip abduction angle increased in the 0 %–35 % ($p = 0.001$) and 77 %–98 % ($p = 0.006$) phases. With a 20° restriction, it increased in the 0 %–78 % phase ($p < 0.001$). Knee extension angle increased in the 44 %–100 % phase ($p < 0.001$). With a 20° restriction, the knee flexion angle increased in the 0 %–23 % phase ($p = 0.005$). Knee abduction angle decreased in the 0 %–55 % phase ($p < 0.001$) and increased in the 76 %–100 % phase ($p = 0.001$). For the results of the joint angular velocity, as the ankle joint restriction angle increased, ankle dorsiflexion angular velocity increased in the 0 %–19 % phase ($p < 0.001$) and ankle plantarflexion angular velocity increased in the 47 %–80 % phase ($p < 0.001$). Hip extension angular velocity increased in the 12 %–18 % ($p = 0.013$) and 67 %–85 % ($p < 0.001$) phases, and hip flexion angular velocity increased in the 30 %–38 % phase ($p = 0.008$). With a 20° restriction, hip extension angular velocity increased in the 41 %–67 % phase ($p < 0.001$). Knee flexion angular velocity increased in the 0 %–12 % phase ($p = 0.002$) and knee extension angular velocity increased in the

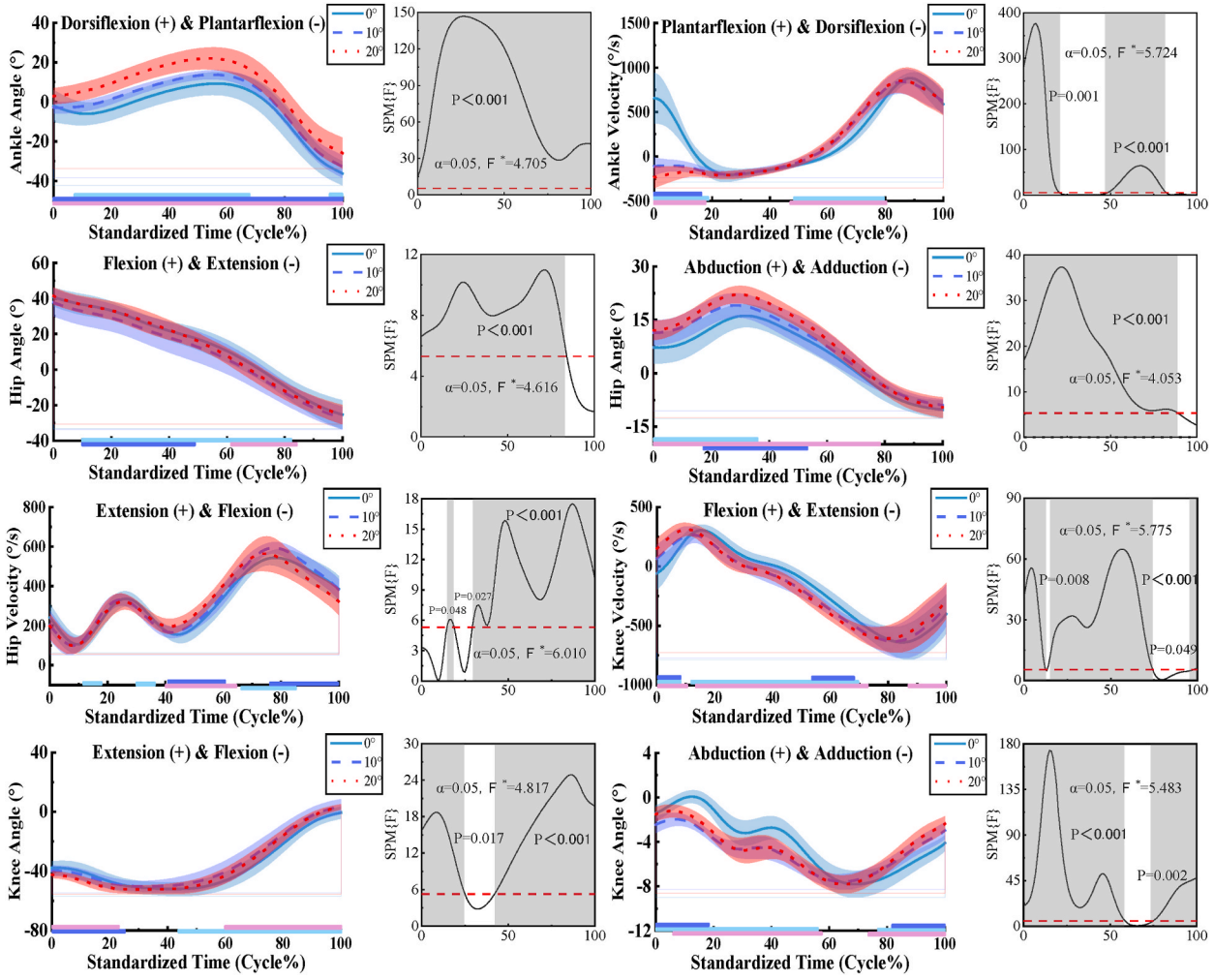

Fig. 4. Kinematics of the ankle, knee, and hip joints during the long jump takeoff. The results of the SPM for NW, 10W and 20W are shown in the Figure. The blue, red, and purple lines represent the results of the SPM analyses for NW and 10W, 10W and 20W, NW and 20W, respectively.

15 %–73 % phase ($p < 0.001$). With a 20° restriction, knee flexion angular velocity increased in the 89 %–100 % phase ($p < 0.001$). Details results of kinematics are provided in Fig. 4.

Ankle dorsiflexion angle and angular velocity ($p < 0.001$), ankle plantarflexion angle and angular velocity ($p < 0.001$, $p = 0.007$ respectively), hip flexion angle ($p = 0.011$), hip extension angle and angular velocity ($p = 0.003$, $p < 0.001$ respectively), hip adduction angle and adduction angle ($p = 0.047$, $p < 0.001$ respectively), knee flexion angle ($p = 0.002$), knee extension angle and angular velocity ($p < 0.001$, $p = 0.005$ respectively), knee adduction angle ($p < 0.001$) were significantly different between NW, 10W, and 20W. Details results of peak kinematics are provided in Table 1. Ankle dorsiflexion and plantarflexion angles differed significantly in all conditions. Hip extension and abduction angles differed significantly in all conditions. Hip extension angular velocity differed significantly between NW and 10W. Knee extension and abduction angles differed significantly in all conditions. Details results of the intergroup differences in peak kinematics are provided in **Supplemental Text and Figures** Fig. 1.

3.2. Kinetics

For the results of the joint moment, as the ankle joint restriction angle increased, the ankle dorsiflexion moment increased in the 0 %–90 % phase ($p < 0.001$). Hip flexion moment increased in the 62 %–100 % phase ($p < 0.001$) and hip extension moment increased in the 0 %–12 % ($p < 0.001$) and 22 %–25 % ($p = 0.012$) phases. With a 20° restriction, knee flexion moment increased in the 0 %–30 % phase ($p < 0.001$) and knee extension moment increased in the 50 %–86 % phase ($p < 0.001$). For the results of the joint power, as the ankle joint restriction angle increased, ankle plantarflexion power increased in the 0 %–3 % ($p = 0.011$) and 10 %–35 % ($p < 0.001$) phases, and ankle dorsiflexion power increased in the 5 %–11 % and 50 %–67 % phases ($p < 0.001$). With a 20° restriction, ankle dorsiflexion power increased in the 50 %–100 % phase ($p < 0.001$). With a 10° restriction, hip flexion power increased in the 0 %–18 % phase ($p < 0.001$), and hip extension power increased in the 20 %–85 % phase ($p < 0.001$). With a 20° restriction, hip flexion power increased in the 0 %–20 % ($p < 0.001$), 40 %–48 % ($p = 0.011$), and 85 %–95 % ($p < 0.001$) phases, and hip extension power increased in the 32 %–38 % ($p = 0.002$) and 50 %–85 % ($p < 0.001$) phases. Knee flexion power increased in the 0 %–15 % and 67 %–94 % phases ($p < 0.001$) and knee extension power increased in the 40 %–60 % phase ($p < 0.001$). With a 10° restriction, knee extension power increased in the 15 %–28 % phase. Details results of kinetic are provided in Fig. 5A.

For the results of ankle joint force, as the ankle restriction angle increased, ankle dorsiflexion joint forces increased in the 0 %–19 % ($p < 0.001$) and 33 %–45 % ($p = 0.001$) phases, and in the 82 %–94 % phase with a 20° restriction ($p < 0.001$). Ankle plantarflexion joint forces increased in the 23 %–29 % phase ($p = 0.014$). Ankle adduction joint forces increased in the 2 %–21 % phase ($p = 0.001$) and the 0 %–35 % phase with a 20° restriction ($p < 0.001$). Ankle abduction joint forces increased in the 42 %–100 % phase ($p < 0.001$), and in the 54 %–100 % phase with a 20° restriction ($p < 0.001$). For the results of the hip joint force, as the ankle restriction angle increased, hip flexion joint forces increased in the 14 %–30 % and 45 %–82 % phases ($p < 0.001$). Hip extension joint forces increased in the 0 %–20 % and 26 %–100 % phases ($p < 0.001$) with a 20° restriction. Hip adduction joint forces increased in the 0 %–10 % ($p < 0.001$), 17 %–23 % ($p = 0.001$), and 70 %–81 % ($p = 0.001$) phases with a 20° restriction. Hip abduction joint forces increased in the 90 %–100 % phase ($p < 0.001$). For the results of knee joint force, as the ankle restriction angle increased, knee flexion joint forces increased in the 0 %–23 % and 74 %–87 % phases ($p < 0.001$), and in the 0 %–82 % phase with a 20° restriction ($p < 0.001$). Knee extension joint forces increased in the 85 %–95 % phase ($p = 0.004$). Knee adduction joint forces increased in the 0 %–5 % ($p = 0.01$) and 83 %–90 % ($p = 0.003$) phases, and in the 0 %–3 % ($p = 0.014$) and 82 %–95 % ($p = 0.001$) phases with a 20° restriction. Knee abduction joint forces increased in the 15 %–70 % ($p < 0.001$) and 25 %–79 % ($p < 0.001$) phases with a 20° restriction. Details results of joint force are provided in Fig. 5B.

Ankle dorsiflexion moment and power ($p < 0.001$), ankle plantarflexion moment ($p < 0.001$), hip flexion power ($p < 0.001$), knee

Table 1
Detailed results of peak joint angles and angular velocities of subjects performing long jump take-off at NW, 10W and 20W.

Parameters	Peak Value	NW Mean ± SD	10W Mean ± SD	20W Mean ± SD	P - Value	F	ES
Ankle	Dorsiflexion	6.93 ± 2.83	13.90 ± 2.35	19.70 ± 2.47	<0.001*	297.613	0.879
Angle (°)	Plantarflexion	−39.70 ± 4.71	−32.81 ± 5.78	−29.00 ± 6.88	<0.001*	37.811	0.654
Ankle	Dorsiflexion	−218.40 ± 61.50	−226.87 ± 30.45	−277.67 ± 80.63	<0.001*	11.528	0.259
Velocity (°/s)	Plantarflexion	880.48 ± 96.79	840.81 ± 163.75	853.03 ± 116.92	0.007*	5.320	0.139
Hip	Flexion	40.48 ± 5.89	37.82 ± 7.77	41.38 ± 4.82	0.011*	4.652	0.074
Angle (°)	Extension	−24.15 ± 8.82	−27.05 ± 6.29	−25.28 ± 5.43	0.003*	6.088	0.095
	Adduction	−10.10 ± 2.50	−9.03 ± 1.56	−9.61 ± 2.87	0.047*	3.296	0.136
	Abduction	15.29 ± 2.65	19.27 ± 3.50	21.80 ± 2.75	<0.001*	86.766	0.790
Hip	Flexion	92.08 ± 38.69	94.06 ± 44.33	94.17 ± 38.15	0.978	0.023	0.001
Velocity (°/s)	Extension	561.22 ± 35.31	602.90 ± 27.96	568.14 ± 89.48	<0.001*	12.597	0.534
Knee	Flexion	−52.64 ± 3.32	−50.29 ± 2.62	−52.30 ± 3.03	0.002*	8.233	0.370
Angle (°)	Extension	−0.54 ± 2.99	3.50 ± 3.15	3.34 ± 1.81	<0.001*	26.587	0.478
	Adduction	−7.82 ± 1.22	−7.66 ± 0.70	−8.01 ± 0.84	0.065	3.031	0.183
	Abduction	0.11 ± 0.61	−1.93 ± 0.52	−1.22 ± 0.60	<0.001*	94.071	0.771
Knee	Flexion	320.36 ± 49.33	311.07 ± 55.20	327.76 ± 52.71	0.302	1.215	0.027
Velocity (°/s)	Extension	−683.89 ± 149.28	−684.44 ± 122.72	−629.31 ± 101.41	0.005*	5.890	0.215

Note: "*" indicates a significant difference ($p < 0.05$) between NW, 10W, and 20W in the take-off phase of the long jump.

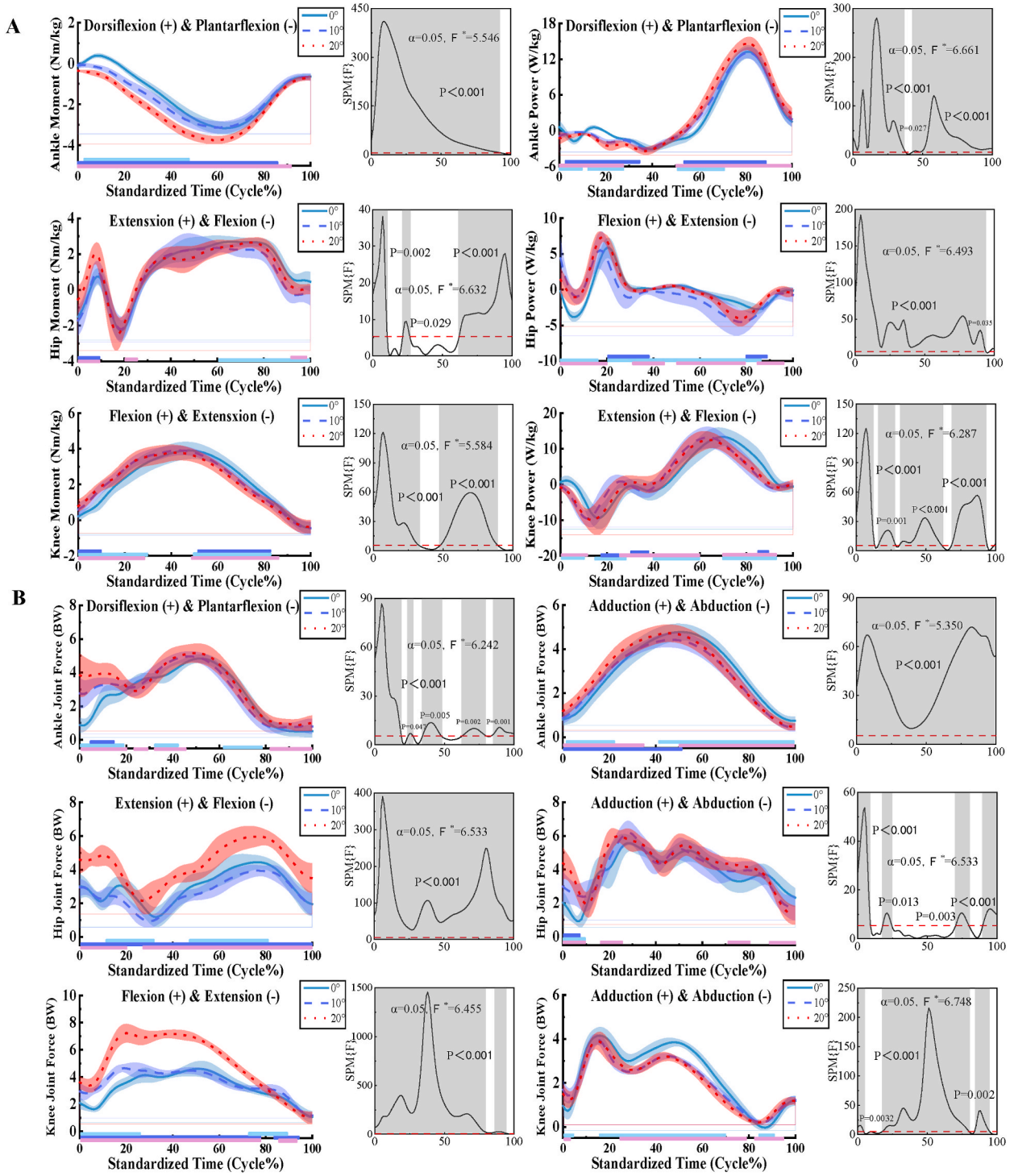

Fig. 5. **(A)** Kinetics of the ankle, knee, and hip joints during the long jump takeoff. **(B)** Joint force during the long jump takeoff. SPM results for NW, 10W and 20W are shown in the Figure. The blue, red and purple lines represent the results of SPM analysis for NW and 10W, 10W and 20W, and NW and 20W, respectively.

extension moment and power ($p = 0.03$, $p = 0.002$ respectively) were significantly different between NW, 10W, and 20W. Knee flexion joint force ($p < 0.001$), and knee extension joint force ($p < 0.001$) were significantly different between NW, 10W, and 20W. Details results of peak kinematics are provided in Tables 2 and 3. Ankle dorsiflexion moments differed significantly in all conditions. Knee extension moments differed significantly between NW and 10W, and between 10W and 20W. Ankle dorsiflexion power and knee

extension power differed significantly between NW and 20W and between 10W and 20W. Ankle plantarflexion, adduction, and abduction joint forces differed significantly in all conditions, and ankle dorsiflexion joint force differed significantly between NW and 20W, and between 10W and 20W. Hip extension joint forces differed significantly in all conditions. Knee flexion joint forces differed significantly between NW and 20W, and between 10W and 20W, and knee abduction joint forces differed significantly between NW and 10W, and between NW and 20W. Details results of the intergroup differences in peak kinematics are provided in **Supplemental Text and Figures** Figs. 2 and 3.

3.3. Muscle activation and muscle co-activation

For the results of the muscle activation, as the ankle restriction angle increased, biceps femoris activation decreased in the 0 %–18 % phase ($p < 0.001$). Rectus femoris activation increased in the 10 %–20 % ($p = 0.006$) and 35 %–55 % ($p < 0.001$) phases but decreased in the 35 %–55 % phase with a 20° restriction ($p < 0.001$). Vastus medialis activation increased in the 18 %–34 % phase with a 10° restriction ($p < 0.001$), and in the 3 %–30 % ($p < 0.001$) and 85 %–100 % ($p = 0.006$) phases with a 20° restriction. Vastus lateralis activation increased in the 18 %–39 % ($p < 0.001$) and 82 %–96 % ($p = 0.001$) phases with a 10° restriction, and in the 0 %–42 % and 82 %–100 % phases with a 20° restriction ($p < 0.001$). Medial gastrocnemius activation increased in the 0 %–32 % phase ($p < 0.001$) and the 44 %–47 % phase with a 20° restriction ($p = 0.014$). Lateral gastrocnemius activation increased in the 8 %–27 % phase ($p < 0.001$) and in the 0 %–32 % phase with a 20° restriction ($p < 0.001$). Soleus activation increased in the 0 %–28 % and 50 %–80 % phases ($p < 0.001$) but decreased in the 31 %–40 % phase ($p = 0.006$). Tibialis anterior activation increased in the 39 %–48 % phase ($p = 0.008$) and the 37 %–55 % phase with a 20° restriction ($p < 0.001$). Details results of muscle activation are provided in Fig. 6A. As the limiting angle of ankle mobility increases, BF/RF and BF/VM increase then decrease, and SOL/TA and MG/TA decrease then increase. Details results of muscle co-activation are provided in Fig. 6B.

3.4. Muscle force

For the results of the muscle force, as the ankle restriction angle increased, rectus femoris muscle force increased in the 55 %–88 % phase ($p < 0.001$) and in the 3 %–13 % phase with a 20° restriction ($p = 0.002$). Biceps femoris muscle force decreased in the 33 %–53 % phase ($p < 0.001$). Vastus medialis muscle force decreased in the 40 %–56 % phase ($p < 0.001$) but increased in the 17 %–27 % phase ($p = 0.001$) and decreased in the 35 %–58 % phase with a 20° restriction ($p < 0.001$). Vastus lateralis muscle force increased in the 12 %–26 % phase ($p < 0.001$) and decreased in the 34 %–57 % phase with a 20° restriction ($p < 0.001$). Medial gastrocnemius muscle force decreased in the 12 %–19 % ($p = 0.007$) and 32 %–48 % ($p < 0.001$) phases, and in the 12 %–58 % phase with a 20° restriction ($p < 0.001$). Lateral gastrocnemius muscle force decreased in the 24 %–52 % ($p < 0.001$) and 91 %–100 % ($p = 0.003$) phases. Soleus muscle force decreased in the 31 %–60 % phase ($p < 0.001$). Tibialis anterior muscle force decreased in the 10 %–25 % ($p < 0.001$) and 32 %–47 % ($p = 0.001$) phases, and in the 5 %–27 % ($p < 0.001$) and 33 %–46 % ($p = 0.008$) phases with a 20° restriction. Details results of muscle force are provided in Fig. 7.

Biceps femoris muscle force ($p < 0.001$), rectus femoris muscle force ($p < 0.001$), vastus medialis muscle force ($p < 0.001$), vastus lateralis muscle force ($p < 0.001$), medial gastrocnemius muscle force ($p < 0.001$), lateral gastrocnemius muscle force ($p = 0.014$), soleus muscle force ($p < 0.001$), and tibialis anterior muscle force ($p = 0.021$) were significantly different between NW, 10W and 20W. Details results of peak muscle force are provided in Table 4. Vastus medialis and vastus lateralis muscle forces differed significantly in all conditions. Biceps femoris, rectus femoris, and medial gastrocnemius muscle forces differed significantly between NW and 10W, and between NW and 20W. Lateral gastrocnemius muscle force differed significantly between NW and 10W and between 10W and 20W. Soleus and tibialis anterior muscle forces differed significantly between NW and 20W and between 10W and 20W. Details results of the intergroup differences in peak muscle force are provided in **Supplemental Text and** Fig. 4.

Table 2
Detailed results of peak joint moments and peak joint power of subjects performing long jump take-off at NW, 10W and 20W.

Parameters	Peak Value	NW Mean ± SD	10W Mean ± SD	20W Mean ± SD	P - Value	F	ES
Ankle Moment (Nm/kg)	Dorsiflexion	0.39 ± 0.31	−0.07 ± 0.30	−0.35 ± 0.21	<0.001*	52.323	0.674
	Plantarflexion	−3.29 ± 0.27	−3.23 ± 0.07	−3.76 ± 0.19	<0.001*	43.575	0.655
Ankle	Dorsiflexion	13.31 ± 1.11	13.33 ± 0.89	14.58 ± 1.19	<0.001*	12.823	0.293
Power (W/kg)	Plantarflexion	−3.32 ± 0.49	−3.30 ± 0.37	−3.47 ± 0.68	0.383	0.975	0.030
Hip	Flexion	−2.44 ± 0.49	−2.58 ± 0.57	−2.54 ± 0.99	0.771	0.262	0.012
Moment (Nm/kg)	Extension	2.69 ± 0.30	2.93 ± 0.29	2.65 ± 0.35	0.295	1.258	0.057
Hip	Flexion	6.14 ± 1.36	7.53 ± 2.12	7.74 ± 0.62	<0.001*	19.594	0.640
Power (W/kg)	Extension	−4.01 ± 0.61	−4.41 ± 1.53	−4.04 ± 1.12	0.371	1.013	0.042
Knee	Flexion	3.90 ± 0.50	3.89 ± 0.24	3.82 ± 0.44	0.273	1.334	0.053
Moment (Nm/kg)	Extension	−0.52 ± 0.33	−0.46 ± 0.42	−0.37 ± 0.28	0.030*	3.783	0.136
Knee	Flexion	−9.47 ± 3.50	−10.42 ± 2.24	−10.22 ± 3.24	0.314	1.195	0.062
Power (W/kg)	Extension	13.76 ± 2.72	13.61 ± 2.92	12.64 ± 2.24	0.002*	6.583	0.151

Note: "*" indicates a significant difference ($p < 0.05$) between NW, 10W, and 20W in the take-off phase of the long jump.

Table 3
Detailed results of peak joint force for subjects performing long jump take-off at NW, 10W and 20W.

Parameters	Peak Value	NW Mean ± SD	10W Mean ± SD	20W Mean ± SD	P - Value	F	ES
Ankle Joint Force (BW)	Dorsiflexion	4.88 ± 0.28	5.02 ± 0.29	5.36 ± 0.52	<0.001*	10.568	0.370
	Plantarflexion	0.40 ± 0.32	0.60 ± 0.33	0.76 ± 0.35	0.003*	8.083	0.487
	Adduction	4.94 ± 0.29	4.46 ± 0.33	4.74 ± 0.414.94	<0.001*	132.613	0.833
	Abduction	0.65 ± 0.21	0.42 ± 0.18	0.47 ± 0.17	<0.001*	18.581	0.412
Hip	Flexion	0.97 ± 0.55	0.77 ± 0.34	2.26 ± 0.55	<0.001*	67.872	0.731
Joint Force (BW)	Extension	4.93 ± 0.43	4.19 ± 0.33	6.02 ± 0.41	<0.001*	125.587	0.834
	Adduction	5.57 ± 0.44	6.36 ± 0.71	6.44 ± 0.49	0.017*	4.776	0.269
	Abduction	0.73 ± 0.32	1.42 ± 0.63	1.23 ± 0.60	0.006*	6.328	0.327
Knee	Flexion	4.90 ± 0.42	4.88 ± 0.26	7.42 ± 0.44	<0.001*	358.634	0.972
Joint Force (BW)	Extension	1.14 ± 0.35	1.17 ± 0.21	1.02 ± 0.46	0.258	1.399	0.060
	Adduction	4.23 ± 0.35	4.07 ± 0.21	4.09 ± 0.44	0.425	0.909	0.115
	Abduction	−0.07 ± 0.12	0.16 ± 0.08	0.21 ± 0.08	<0.001*	45.578	0.752

Note: "*" indicates a significant difference ($p < 0.05$) between NW, 10W, and 20W in the take-off phase of the long jump.

3.5. Center of mass, gain in vertical velocity, and loss in horizontal velocity

For the results of the center of mass velocity distribution, as the ankle restriction angle increased, the vertical velocity of the center of mass increased in the 0 %–5 % ($p = 0.016$) and 30 %–60 % ($p < 0.001$) phases, and in the 10 %–18 % ($p = 0.001$) and 22 %–75 % ($p < 0.001$) phases with a 20° restriction. The horizontal velocity of the center of mass increased in the 0 %–5 % ($p = 0.01$), 10 %–30 % ($p < 0.001$), and 90 %–100 % ($p = 0.001$) phases but decreased in the 5 %–10 % ($p = 0.007$), 30 %–60 % ($p < 0.001$), and 80 %–100 % ($p < 0.001$) phases with a 20° restriction. For the results of the center-of-mass position distribution, as the ankle restriction angle increased, center-of-mass heights increased in the 0 %–100 % phase ($p < 0.001$). Center-of-mass offset distances decreased in the 23 %–100 % phase ($p = 0.008$) with a 10° restriction. Details results of the center of mass velocity distribution and position distribution are provided in Fig. 8A.

As the ankle restriction angle increased, the vertical velocity gains during the long jump takeoff were significantly different in all three cases, and the horizontal velocity losses during the long jump takeoff were significantly different between NW and 20W and between 10W and 20W, and there were significant differences in vertical velocity gain ($p < 0.001$) and horizontal velocity loss ($p = 0.002$) between NW, 10W and 20W during the takeoff phase of the long jump. Details results of gain in vertical velocity and loss in horizontal velocity are provided in Table 5 and Fig. 8B.

4. Discussion

The purpose of this study was to investigate the effects of different angles of the pedal (different degrees of ankle dorsiflexion restriction) on lower limb biomechanics during the long jump takeoff. As the ankle dorsiflexion limitation angles increase to 10°, there is a better gain and a lower risk of injury during long jump takeoff. Conversely, failure to significantly improve validation output at a 20° ankle dorsiflexion limitation angle may increase injury risk. There will not be consistently better gains and consistently lower risk of injury with increasing pedal angles that increase ankle dorsiflexion limitation angles.

Our study elucidated several key findings: (1) As the ankle restriction angle increased, the vertical velocity gain of the athlete during the takeoff phase gradually increased, while at the same time, the horizontal velocity loss of the athlete during the takeoff phase did not differ significantly between no NW and 10W. significant difference, rather the horizontal velocity loss increased significantly when the ankle joint restriction angle was increased to 20°. (2) As the ankle joint restriction angle increased, the mean center of mass vertical velocity gradually increased during the jump phase, and the mean center of mass horizontal velocity increased only when the ankle joint restriction angle was increased to 10°, the mean center of mass height gradually increased during the jump phase, and the mean center of mass excursion (displacement of the center of mass in the coronal plane) was minimized when the ankle joint restriction angle was increased to 10°. (3) When the ankle dorsiflexion limiting angle of 10°, the peak extension angle, angular velocity, and power were highest at the knee and hip joints. (4) Joint forces at the hip and knee were greatest when the ankle dorsiflexion restriction angle was 20°.

In the long jump, takeoff velocity is crucial and can be categorized into vertical and horizontal components [36]. Previous studies have shown that achieving maximum gain in vertical velocity from touchdown to takeoff is correlated with specific techniques, including maintaining a low center of gravity, achieving a greater knee angle at touchdown, and exhibiting a low peak knee flexion velocity, which reflects the capacity to resist knee flexion [19,37,38]. To minimize the reduction in horizontal velocity, it is beneficial to reduce hip adduction and increase hip abduction. Strengthening the hip abductors helps achieve the former while emphasizing hip extension during the jump can facilitate the latter. Greater flexibility in hip extension further enhances this capability [19,37,38]. Verification of results showed that as the ankle joint restriction angle increased, the vertical velocity of the center of mass increased, peaking at 20°, while the horizontal velocity peaked at 10° and decreased with higher angles [39]. The overall center of mass velocity decreased with increasing pedal angle. The mean vertical height of the center of mass increased with pedal angle, optimizing jump height [39,40]. Less deflection of the center of mass in the coronal plane with pedals suggests better balance during the jump [2,41]. These findings align with previous research showing that the center of mass displacement increases with velocity, but its inward and

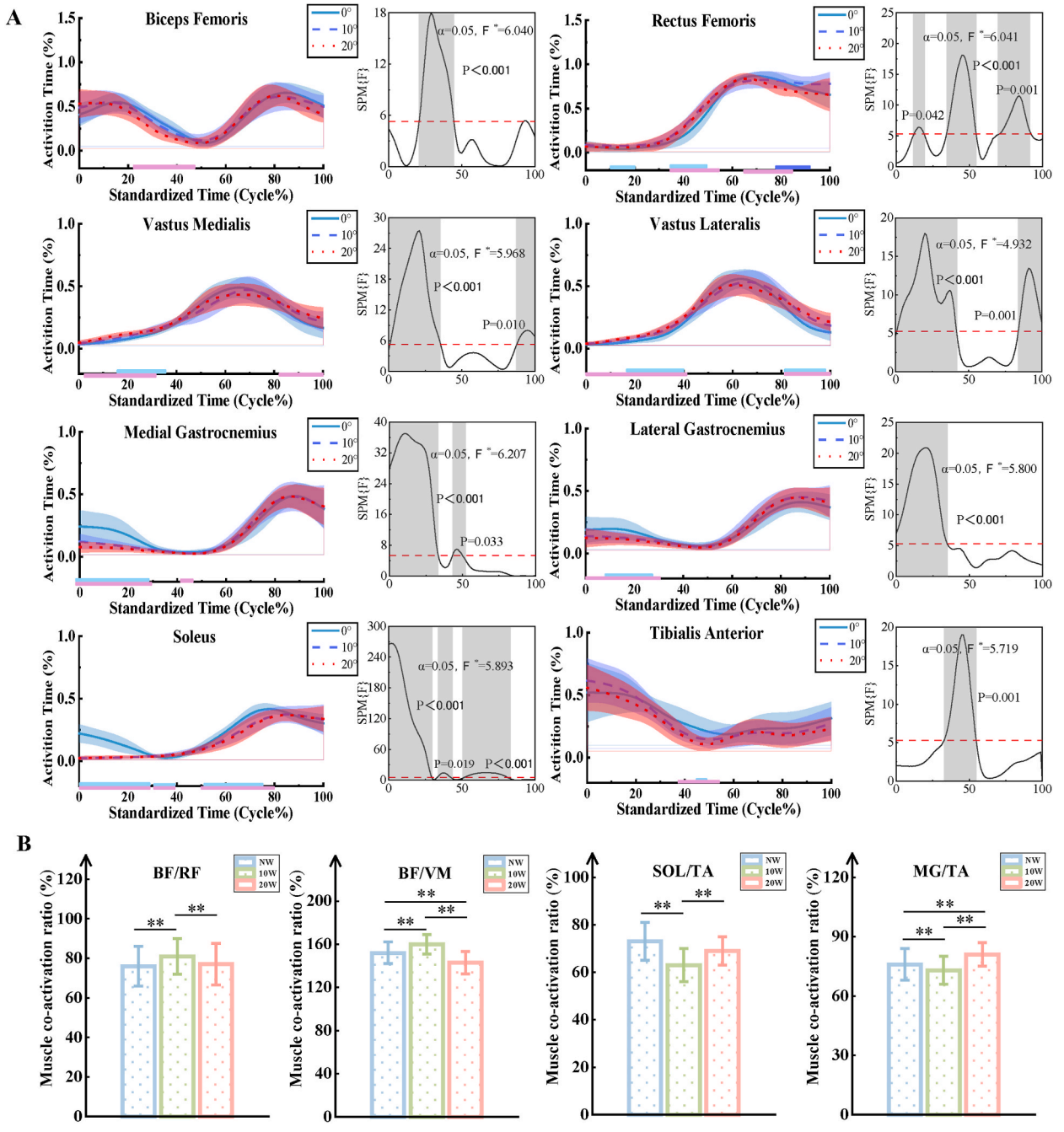

Fig. 6. **(A)** Muscle activation during the long jump takeoff. SPM results for NW, 10W and 20W are shown in the Figure. The blue, red and purple lines represent the results of SPM analysis for NW and 10W, 10W and 20W, and NW and 20W, respectively. **(B)** Lower limb muscle co-activation results during the long jump takeoff. Abbreviations: BF: biceps femoris; RF: rectus femoris; VM: vastus medialis; SOL: soleus; TA: tibialis anterior; MG: medial gastrocnemius.

outward motion decreases [42].

Another important observation is that as the angle of ankle restriction increases, compensatory adjustments such as increased knee and hip extension angles and angular velocities are produced during the jumping phase to increase knee and hip extension power, and these compensatory adjustments may help athletes to overcome the limitations imposed by ankle motion restriction and enhance the athlete's athletic performance. According to the prevailing literature, during the long jump takeoff, athletes aim to minimize flexion of the takeoff leg to optimize spring force following rapid hip extension. Additionally, greater knee extension at touchdown is employed to mitigate knee hyperflexion [43,44]. The jumper should aim to maintain minimal flexion of the takeoff leg knee to maximize spring

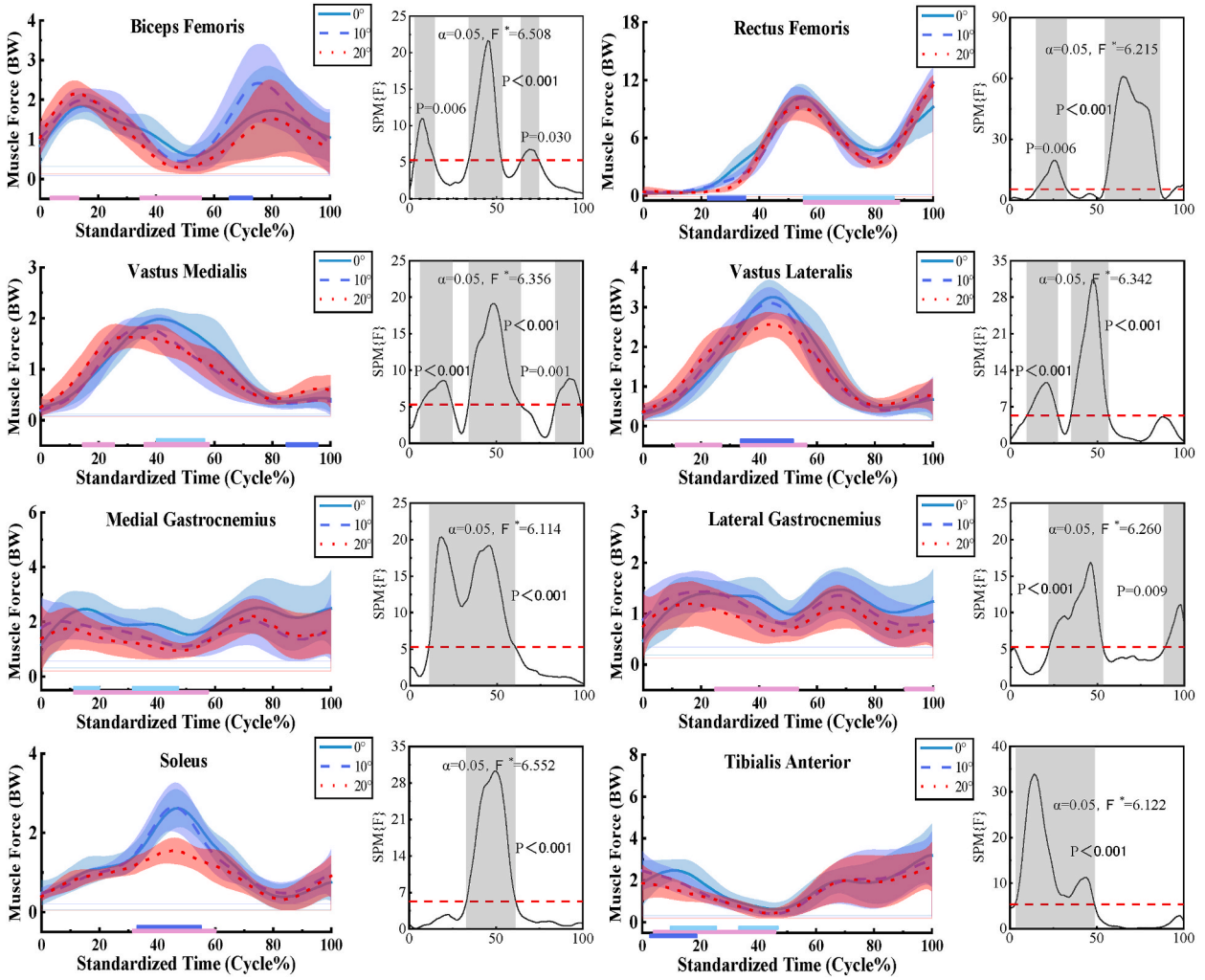

Fig. 7. Muscle force during the long jump takeoff. SPM results for NW, 10W and 20W are shown in the Figure. The blue, red and purple lines represent the results of SPM analysis for NW and 10W, 10W and 20W, and NW and 20W, respectively.

Table 4
Detailed results of peak muscle force for subjects performing long jump take-off at NW, 10W and 20W.

Muscle force parameters (BW)	NW Mean ± SD	10W Mean ± SD	20W Mean ± SD	P - Value	F	ES
Biceps Femoris	2.15 ± 0.60	2.83 ± 0.73	2.53 ± 0.57	<0.001*	8.576	0.335
Rectus Femoris	13.76 ± 1.06	11.89 ± 1.28	11.65 ± 0.69	<0.001*	17.018	0.607
Vastus Medialis	2.05 ± 0.15	1.95 ± 0.21	1.80 ± 0.24	<0.001*	11.476	0.353
Vastus Lateralis	3.45 ± 0.30	3.20 ± 0.36	2.76 ± 0.33	<0.001*	28.246	0.585
Medial Gastrocnemius	3.66 ± 0.15	2.87 ± 0.98	2.78 ± 0.79	<0.001*	9.507	0.268
Later Gastrocnemius	1.91 ± 0.30	1.84 ± 0.36	1.51 ± 0.41	0.014*	5.159	0.310
Soleus	2.91 ± 0.47	2.87 ± 0.58	1.70 ± 0.31	<0.001*	41.729	0.723
Tibialis Anterior	3.94 ± 0.96	3.78 ± 1.17	3.31 ± 1.02	0.021*	4.043	0.096

Note: "*" indicates a significant difference ($p < 0.05$) between NW, 10W, and 20W in the take-off phase of the long jump.

force following rapid hip extension. Additionally, employing greater knee extension at touchdown helps prevent excessive knee flexion [45]. In this study, different from previous studies, with the increase of ankle dorsiflexion angle, the knee joint showed greater flexion Angle and flexion angular velocity in the buffer phase, and greater extension speed in the pushout phase. This may be due to a compensatory mechanism produced by athletes after the ankle dorsiflexion range of motion is limited. Due to the limited ankle dorsiflexion, greater knee flexion is used for cushioning, and equal knee extension is used to compensate for the reduced ankle dorsiflexion range of motion to achieve better athletic performance. It has also been shown that limiting ankle range of motion prevents

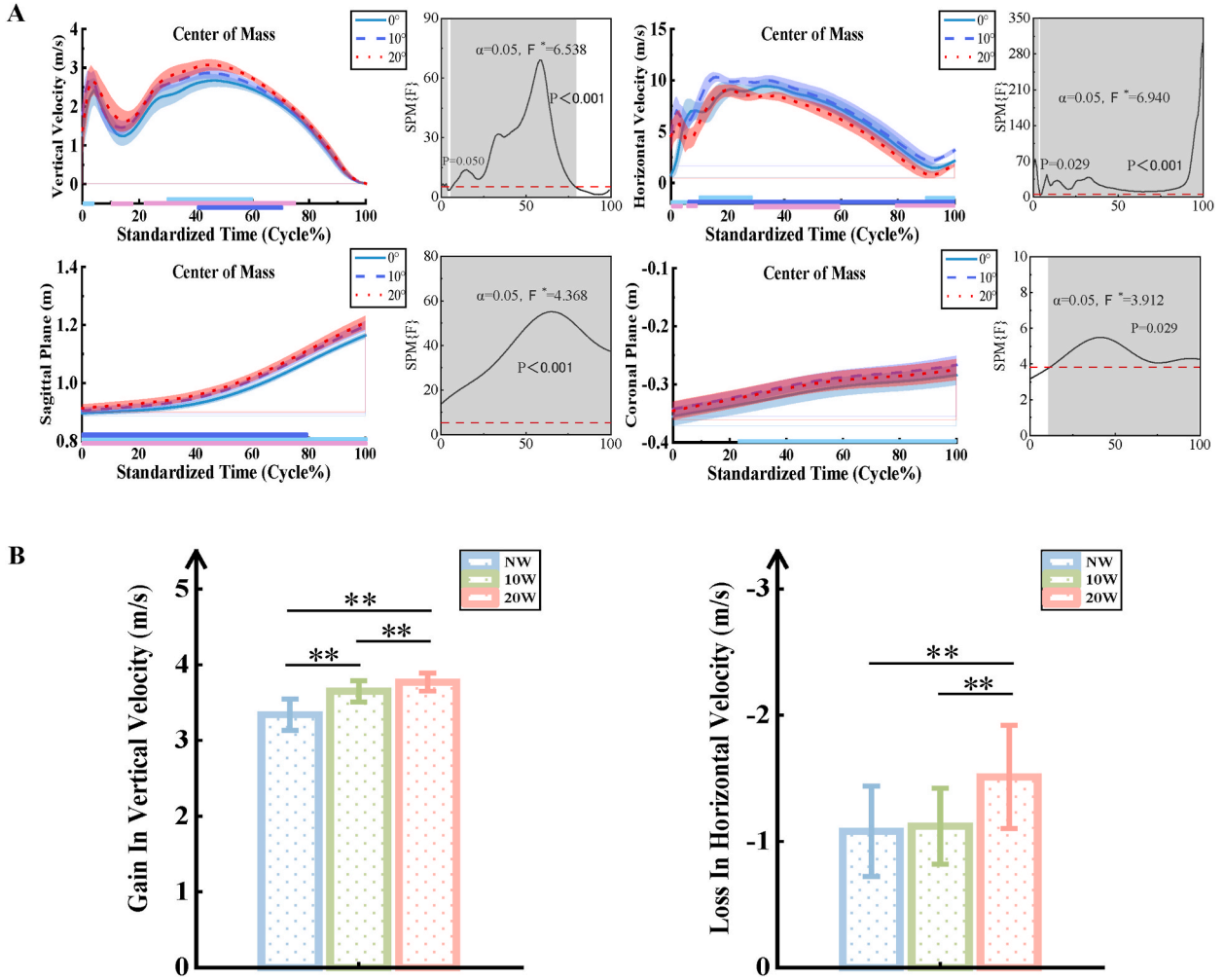

Fig. 8. **(A)** Center of mass velocity distribution and position distribution during the long jump takeoff. SPM results for NW, 10W and 20W are shown in the Figure. The blue, red and purple lines represent the results of SPM analysis for NW and 10W, 10W and 20W, and NW and 20W, respectively. **(B)** Between-group differences in vertical velocity gain and horizontal velocity loss results at the ankle, knee, and hip joints for NW, 10W, and 20W jumps, respectively. Note: "*" indicates a significant difference between NW, 10W and 20W ($p < 0.05$).

Table 5
Detailed results of gain in vertical velocity and loss in horizontal velocity for subjects performing long jump at NW, 10W and 20W.

Parameters	NW Mean ± SD	10W Mean ± SD	20W Mean ± SD	P - Value	F	ES
Gain In Vertical Velocity (m/s)	3.34 ± 0.21	3.65 ± 0.14	3.77 ± 0.12	<0.001*	43.131	0.683
Loss In Horizontal Velocity (m/s)	−1.08 ± 0.36	−1.12 ± 0.30	−1.51 ± 0.41	0.002*	7.087	0.262

Note: "*" indicates a significant difference ($p < 0.05$) between NW, 10W, and 20W in the take-off phase of the long jump.

subjects from using correct postural strategies during postural tasks [46], but it is possible that during dynamic tasks where ankle range of motion is limited, the athlete may be able to use a more extended knee to move better being limited and adaptive changes produced by the athlete for better motor performance.

Joint stability is fundamentally influenced by muscle co-activation. Impaired muscle co-activation can significantly compromise knee stability. The pattern of muscle co-activation surrounding the knee joint is crucial for providing dynamic knee stability and preventing injuries. Muscle co-activation is instrumental in converting valgus forces into joint contact forces, thereby protecting the knee from potential injuries. Building on previous research, our study meticulously analyzed and quantified the muscle co-activation patterns around the knee joints of our participants [33]. Extant literature underscores that the stability of lower limb joints is heavily contingent upon the coordinated co-activation of muscles [47,48]. Limitation of ankle joint mobility results in decreased activation of the soleus (SOL) and gastrocnemius (MG) muscles, accompanied by increased activation of the tibialis anterior (TA) muscle. Our

findings indicate that with increasing ankle mobility restriction, the ratios of SOL/TA and MG/TA initially decrease and then increase, while the ratios of biceps femoris (BF)/rectus femoris (RF) and BF/vastus medialis (VM) initially increase and then decrease. These changes suggest that knee stability and muscle control are enhanced when ankle dorsiflexion is limited to an angle of 10° during long jump initiation. This observation is consistent with prior research, which posits that coordinated knee muscle activation enhances joint stiffness and protects the ACL from injury by transforming valgus forces into joint contact forces [49].

Previous research has demonstrated that excessive joint stress can lead to joint pain, stiffness, and impaired mobility [50,51]. Our results found that knee forces tended to increase significantly during jumping as the pedal angle increased, with an optimal equilibrium of knee forces when jumping on 10° ankle dorsiflexion angle, contributing to lower limb stability and efficiency of force transfer, and a significant increase in knee forces when jumping on 20° ankle dorsiflexion angle, which may lead to overstressing of the knee joint and impaired mobility. This can lead to excessive stress on the knee joint, increasing the risk of injury, as well as ankle forces and hip forces [50,51]. Previous studies have shown that excessive joint pressure can lead to joint pain, stiffness, and impaired mobility [51,52]. Our results found a significant increase in knee force when the ankle dorsiflexion Angle was 20°, which may lead to excessive stress and impaired mobility of the knee. This can lead to excessive stress on the knee joint, increasing the risk of injury, as well as ankle and hip forces. However, previous studies only focused on the sagittal joint force without the coronal plane. In this study, the joint forces of the ankle joint, knee joint, and hip joint in the coronal plane were also investigated. Among them, the knee joint showed the most obvious changes. It is worth noting that the muscles surrounding the knee joint play an important role in biomechanical alterations and joint instability, including the strength of the quadriceps [53,54], hamstrings, and gastrocnemius [55], and that knee loading is determined by the interactions of the quadriceps, hamstrings, gastrocnemius, and piriformis muscles [15], and that on a 20° pedal The muscular strength of these muscles decreases significantly during jumping, which may significantly cause a decrease in joint stability leading to injury. Therefore, a rational choice of pedal angle is important both from the point of view of improving athletic performance and preventing sports injuries.

One of the key strengths of this study is the use of OpenSim, a sophisticated musculoskeletal modeling software that allows for the construction of subject-specific models by scaling a generic template based on each participant's anatomical measurements. This ensures that the simulations closely reflect the participants' actual biomechanics, leading to more accurate and personalized analyses. OpenSim enables the computation of joint forces, muscle activations, and joint moments using data from the Vicon motion capture system and AMTI force platform, providing a deeper understanding of the internal biomechanical responses to different dorsiflexion restrictions. This level of precision is critical for identifying subtle changes in joint loading and muscle coordination, which might not be detectable with surface-level kinematic data alone. By utilizing tools like Inverse Kinematics and Static Optimization algorithms, the study was able to simulate muscle forces and joint moments during the takeoff phase, offering detailed insights into how different dorsiflexion restrictions impact lower limb joint forces, particularly at the ankle, knee, and hip joints, which are vital for performance optimization and injury prevention.

To maximize the reduction of experimental error, the athletes selected in this study were all Division IIlevel long jumper athletes who were fully warmed up before the test. To simulate the real competition level, each subject tried jumping six times at each Angle. To prevent excessive fatigue from affecting the test results, adequate rest was taken between each group. However, there are several limitations to the current study, this study was conducted under laboratory conditions which may differ from the actual competitive environment. Future studies should consider conducting experiments in conditions that simulate actual competition to improve the external validity of the findings. At the same time unifying the gender may reduce the influence of confounding factors, such as the technical characteristics of jumping between men and women, while our study included 30 male long jumpers at the Division II level, the sample size, while potentially sufficient for some analyses, may require a larger group and different genders as well as other athletic level grades to improve statistical power and generalizability of results. At the same time, the flexibility of the ankle joint, the strength of lower limb muscles, the strength of the hip and core, as well as the height and limb length of participants may be different among each athlete, which is also a problem that needs to be solved in future studies. Therefore, it is suggested that athletes should refer to their own conditions during training to select the ankle dorsiflexion limitation angle, which can also be understood as a reasonable choice of pedal angle.

5. Conclusion

The results of the study showed that athletes jumping at an ankle dorsiflexion restriction angle of about 10° had an increase in vertical velocity with minimal loss of horizontal velocity, and these conditions may allow athletes to achieve faster jumping speeds and be more favorable for improving their long jump performance. In addition, co-activation of the muscles around the knee joint was higher when jumping with an ankle dorsiflexion restriction angle of approximately 10°, which may contribute to improved knee stability during long jump initiation. The present study suggests that athletes should limit ankle dorsiflexion to about 10° during long jump training to increase jumping speed, improve technical movements and long jump performance, and minimize the risk of injury.

STAR★Methods

Resource Availability

Lead contact

Further information and requests for resources and data should be directed to and will be fulfilled by the Lead Contact, Yaodong Gu (guyaodong@nbu.edu.cn).

CRediT authorship contribution statement

Zanni Zhang: Writing – original draft, Visualization, Methodology, Investigation, Data curation. **Datao Xu:** Validation, Supervision, Investigation, Conceptualization. **Xiangli Gao:** Visualization, Data curation. **Huiyu Zhou:** Visualization, Validation, Supervision, Data curation. **Julien S. Baker:** Writing – review & editing, Formal analysis. **Zsolt Radak:** Writing – review & editing, Formal analysis. **Yaodong Gu:** Writing – review & editing, Supervision, Funding acquisition, Conceptualization.

Data availability

- All data pertinent to this study are included in the article,
- Any additional information required to re-analyze the data reported in this paper is available from the lead contact upon request

Declaration of Competing interest

We declare that we have no financial and personal relationships with other people or organizations that can inappropriately influence our work, there is no professional or other personal interest of any nature or kind in any product, service and/or company that could be construed as influencing the position presented in, or the review of, the manuscript entitled, "***Differences of simulated ankle dorsiflexion limitation on lower extremity biomechanics during long jump takeoff***".

Acknowledgements

This study was sponsored by Zhejiang Provincial Natural Science Foundation of China for Distinguished Young Scholars (LR22A020002), Zhejiang Provincial Key Research and Development Program of China (2023C03197), Ningbo key R&D Program (2022Z196), Zhejiang Province Exploring Public Welfare Projects (LTGY23H040003), Ningbo Natural Science Foundation (20221JCGY010532, 20221JCGY010607), Public Welfare Science & Technology Project of Ningbo, China (2021S134), and Zhejiang Rehabilitation Medical Association Scientific Research Special Fund (ZKKY2023001). We express our heartfelt gratitude for this.

Appendix ASupplementary data

Supplementary data to this article can be found online at https://doi.org/10.1016/j.heliyon.2024.e41009.

References

[1] V. Jasminan, A. Chandana, Two dimensional analysis of changes in athlete's center of mass during the long jump flight phase, International Journal of Research in Engineering and Innovation 5 (2021) 154–158, https://doi.org/10.36037/IJREI.2021.5304.
[2] A.S. Theodorou, V. Panoutsakopoulos, T.A. Exell, P. Argeitaki, G.P. Paradisis, A. Smirniotou, Step characteristic interaction and asymmetry during the approach phase in long jump, J. Sports Sci. 35 (2017) 346–354, https://doi.org/10.1519/JSC.0000000000000849.
[3] W. Kakihana, S. Suzuki, The EMG activity and mechanics of the running jump as a function of takeoff angle, J. Electromyogr. Kinesiol. 11 (2001) 365–372, https://doi.org/10.1016/S1050-6411(01)00008-6.
[4] H. Koyama, Y. Muraki, M. Ae, Athletics: effects of an inclined board as a training tool on the take-off motion of the long jump, Sports BioMech. 4 (2005) 113–129, https://doi.org/10.1080/14763140508522858.
[5] N.P. Linthorne, M.S. Guzman, L.A. Bridgett, Optimum takeoff angle in the long jump, J. Sports Sci. 23 (2005) 703–712, 1080/02640410400022011.
[6] Y. Kwon, G. Shin, Foot kinematics and leg muscle activation patterns are altered in those with limited ankle dorsiflexion range of motion during incline walking, Gait Posture 92 (2022) 315–320, https://doi.org/10.1016/j.gaitpost.2021.12.002.
[7] A. Mason-Mackay, C. Whatman, D. Reid, The effect of reduced ankle dorsiflexion on lower extremity mechanics during landing: a systematic review, J. Sci. Med. Sport 20 (2017) 451–458, https://doi.org/10.1016/j.jsams.2015.06.006.
[8] D. Xu, H. Zhou, W. Quan, X. Ma, T.-E. Chon, J. Fernandez, F. Gusztav, A. Kovács, J.S. Baker, Y. Gu, New insights optimize landing strategies to reduce lower limb injury risk, Cyborg and Bionic Systems 5 (2024) 126, https://doi.org/10.34133/cbsystems.0126.
[9] D. Xu, H. Zhou, W. Quan, F. Gusztav, M. Wang, J.S. Baker, Y. Gu, Accurately and effectively predict the ACL force: utilizing biomechanical landing pattern before and after-fatigue, Comput. Methods Progr. Biomed. 241 (2023) 107761, https://doi.org/10.1016/j.cmpb.2023.107761.
[10] J.B. Taylor, E.S. Wright, J.P. Waxman, R.J. Schmitz, J.D. Groves, S.J. Shultz, Ankle dorsiflexion affects hip and knee biomechanics during landing, Sports health 14 (2022) 328–335, https://doi.org/10.1177/19417381211019683.
[11] I. Godinho, B.N. Pinheiro, L.D.S. Júnior, G.C. Lucas, J.F. Cavalcante, G.M. Monteiro, P.A.G. Uchoa, Effect of reduced ankle mobility on jumping performance in young athletes, Motricidade 15 (2019) 46–51, https://doi.org/10.6063/motricidade.12869.
[12] S. Ota, M. Ueda, K. Aimoto, Y. Suzuki, S. Sigward, Acute influence of restricted ankle dorsiflexion angle on knee joint mechanics during gait, Knee 21 (2014) 669–675, https://doi.org/10.1016/j.knee.2014.01.006.
[13] A.A. Vandervoort, Ankle mobility and postural stability, Physiotherapy theory and practice 15 (1999) 91–103, https://doi.org/10.1080/095939899307793.
[14] L.J. Backman, P. Danielson, Low range of ankle dorsiflexion predisposes for patellar tendinopathy in junior elite basketball players: a 1-year prospective study, Am. J. Sports Med. 39 (2011) 2626–2633, https://doi.org/10.1177/03635465114205.
[15] T. Van Eijden, W. De Boer, W. Weijs, The orientation of the distal part of the quadriceps femoris muscle as a function of the knee flexion-extension angle, J. Biomech. 18 (1985) 803–809.
[16] D. Xu, W. Quan, H. Zhou, D. Sun, J.S. Baker, Y. Gu, Explaining the differences of gait patterns between high and low-mileage runners with machine learning, Sci. Rep. 12 (2022) 2981, https://doi.org/10.1038/s41598-022-07054-1.
[17] D. Xu, H. Zhou, W. Quan, X. Jiang, M. Liang, S. Li, U.C. Ugbolue, J.S. Baker, F. Gusztav, X. Ma, A new method proposed for realizing human gait pattern recognition: Inspirations for the application of sports and clinical gait analysis, Gait Posture 107 (2024) 293–305, https://doi.org/10.1016/j.gaitpost.2023.10.019.

[18] A. Seyfarth, R. Blickhan, J.V. Leeuwen, Optimum takeoff techniques and muscle design for long jump, J. Exp. Biol. 203 (2000) 741–750, https://doi.org/10.1242/jeb.203.4.741.
[19] P. Graham-Smith, A. Lees, A three-dimensional kinematic analysis of the long jump takeoff, J. Sports Sci. 23 (2005) 891–903, https://doi.org/10.1080/02640410400022169.
[20] L.A. Bridgett, N.P. Linthorne, Changes in long jump takeoff technique with increasingrun-up speed, J. Sports Sci. 24 (2006) 889–897, https://doi.org/10.1080/02640410500298040.
[21] J.G. Hay, J.A. Miller, Techniques used in the transition from approach to takeoff in the long jump, J. Appl. Biomech. 1 (1985) 174–184, https://doi.org/10.1123/ijsb.1.2.174.
[22] H. Kang, Sample size determination and power analysis using the G* Power software, Journal of educational evaluation for health professions 18 (2021), https://doi.org/10.3352/jeehp.2021.18.17.
[23] D. Xu, J. Lu, J.S. Baker, G. Fekete, Y. Gu, Temporal kinematic and kinetics differences throughout different landing ways following volleyball spike shots, Proc. Inst. Mech. Eng. P J. Sports Eng. Technol. 236 (2022) 200–208, https://doi.org/10.1177/17543371211009485.
[24] W.K. Lam, R. Ding, Y. Qu, Ground reaction forces and knee kinetics during single and repeated badminton lunges, J. Sports Sci. 35 (2017) 587–592, https://doi.org/10.1080/02640414.2016.1180420.
[25] D. Xu, H. Zhou, M. Wang, F. Gusztav, T.-E. Chon, J. Fernandez, J.S. Baker, Y. Gu, Contribution of ankle motion pattern during landing to reduce the knee-related injury risk, Comput. Biol. Med. 180 (2024) 108965, https://doi.org/10.1016/j.compbiomed.2024.108965.
[26] H.J. Hermens, B. Freriks, C. Disselhorst-Klug, G. Rau, Development of recommendations for SEMG sensors and sensor placement procedures, J. Electromyogr. Kinesiol. 10 (2000) 361–374, https://doi.org/10.1016/S1050-6411(00)00027-4.
[27] F. Panteli, C. Tsolakis, D. Efthimiou, A. Smirniotou, Acquisition of the long jump skill, using different learning techniques, Sport Psychol. 27 (2013) 40–52, https://doi.org/10.1123/tsp.27.1.40.
[28] R.J. Butler, J.D. Willson, D. Fowler, R.M. Queen, Gender differences in landing mechanics vary depending on the type of landing, Clin. J. Sport Med. 23 (2013) 52–57, https://doi.org/10.1097/JSM.0b013e318259efa0.
[29] C.A. Myers, D. Hawkins, Alterations to movement mechanics can greatly reduce anterior cruciate ligament loading without reducing performance, J. Biomech. 43 (2010) 2657–2664, https://doi.org/10.1016/j.jbiomech.2010.06.003.
[30] B. Yu, C.-F. Lin, W.E. Garrett, Lower extremity biomechanics during the landing of a stop-jump task, Clin. Biomech. 21 (2006) 297–305, https://doi.org/10.1016/j.clinbiomech.2005.11.003.
[31] A. Rajagopal, C.L. Dembia, M.S. DeMers, D.D. Delp, J.L. Hicks, S.L. Delp, Full-body musculoskeletal model for muscle-driven simulation of human gait, IEEE Trans. Biomed. Eng. 63 (2016) 2068–2079, https://doi.org/10.1109/TBME.2016.2586891.
[32] S.L. Delp, F.C. Anderson, A.S. Arnold, P. Loan, A. Habib, C.T. John, E. Guendelman, D.G. Thelen, OpenSim: open-source software to create and analyze dynamic simulations of movement, IEEE Trans. Biomed. Eng. 54 (2007) 1940–1950, https://doi.org/10.1109/TBME.2007.901024.
[33] G. Márquez, X. Aguado, L.M. Alegre, M. Férnandez-del-Olmo, Neuromechanical adaptation induced by jumping on an elastic surface, J. Electromyogr. Kinesiol. 23 (2013) 62–69, https://doi.org/10.1016/j.jelekin.2012.06.012.
[34] C.J. De Luca, L.D. Gilmore, M. Kuznetsov, S.H. Roy, Filtering the surface EMG signal: movement artifact and baseline noise contamination, J. Biomech. 43 (2010) 1573–1579, https://doi.org/10.1016/j.jbiomech.2010.01.027.
[35] T.C. Pataky, One-dimensional statistical parametric mapping in Python, Comput. Methods Biomech. Biomed. Eng. 15 (2012) 295–301, https://doi.org/10.1080/10255842.2010.527837.
[36] R.M. Alexander, Optimum takeoff techniques for high and long jumps, Philosophical Transactions of the Royal Society of London. Series B: Biological Sciences 329 (1990) 3–10, https://doi.org/10.1098/rstb.1990.0144.
[37] T. Jaitner, L. Mendoza, W. Schöllhorn, Analysis of the long jump technique in the transition from approach to takeoff based on time-continuous kinematic data, Eur. J. Sport Sci. 1 (2001) 1–12, https://doi.org/10.1080/17461390100071506.
[38] J.H. Mettler, R. Shapiro, M.B. Pohl, Effects of a hip flexor stretching program on running kinematics in individuals with limited passive hip extension, J. Strength Condit Res. 33 (2019) 3338–3344, https://doi.org/10.1519/JSC.0000000000002586.
[39] A. Sánchez-Sixto, A.J. Harrison, P. Floría, Larger countermovement increases the jump height of countermovement jump, Sports 6 (2018) 131, https://doi.org/10.3390/sports6040131.
[40] N.A. Bates, K.R. Ford, G.D. Myer, T.E. Hewett, Impact differences in ground reaction force and center of mass between the first and second landing phases of a drop vertical jump and their implications for injury risk assessment, J. Biomech. 46 (2013) 1237–1241, https://doi.org/10.1016/j.jbiomech.2013.02.024.
[41] E.M. Gutierrez-Farewik, Å. Bartonek, H. Saraste, Comparison and evaluation of two common methods to measure center of mass displacement in three dimensions during gait, Human movement science 25 (2006) 238–256, https://doi.org/10.1016/j.humov.2005.11.001.
[42] G. Cavagna, The landing–takeoff asymmetry in human running, J. Exp. Biol. 209 (2006) 4051–4060, https://doi.org/10.1242/jeb.02344.
[43] Y. Muraki, M. Ae, T. Yokozawa, H. Koyama, Athletics: mechanical properties of the take-off leg as a support mechanism in the long jump, Sports BioMech. 4 (2005) 1–15, https://doi.org/10.1080/14763140508522848.
[44] A. Lees, N. Fowler, D. Derby, A biomechanical analysis of the last stride, touch-down and take-off characteristics of the women's long jump, J. Sports Sci. 11 (1993) 303–314, https://doi.org/10.1080/02640419308730000.
[45] T. Jie, J. Li, E.-C. Teo, Limb biomechanical difference between bounced and alternating jumping rope, Int. J. Biomed. Eng. Technol. 29 (2024) 150–163, https://doi.org/10.1504/IJBET.2024.138714.
[46] H.-S. Jeon, S. Hwang, Y.-K. Woo, The effect of ankle and knee immobilization on postural control during standing, Knee 20 (2013) 600–604, https://doi.org/10.1016/j.knee.2012.09.001.
[47] G. Márquez, X. Aguado, L.M. Alegre, M. Férnandez-del-Olmo, Neuromechanical adaptation induced by jumping on an elastic surface, J. Electromyogr. Kinesiol. 23 (2013) 62–69, https://doi.org/10.1016/j.jelekin.2012.06.012.
[48] F. Ramezani, F. Saki, B. Tahayori, Neuromuscular training improves muscle co-activation and knee kinematics in female athletes with high risk of anterior cruciate ligament injury, Eur. J. Sport Sci. 24 (2024) 56–65, https://doi.org/10.1002/ejsc.12046.
[49] T.E. Hewett, M.V. Paterno, G.D. Myer, Strategies for enhancing proprioception and neuromuscular control of the knee, Clin. Orthop. Relat. Res. 402 (2002) 76–94, https://doi.org/10.1097/00003086-200209000-00008, 1976-2007.
[50] J.A. Buckwalter, Sports, joint injury, and posttraumatic osteoarthritis, J. Orthop. Sports Phys. Ther. 33 (2003) 578–588, https://doi.org/10.2519/jospt.2003.33.10.578.
[51] J.A. Buckwalter, D.D. Anderson, T.D. Brown, Y. Tochigi, J.A. Martin, The roles of mechanical stresses in the pathogenesis of osteoarthritis: implications for treatment of joint injuries, Cartilage 4 (2013) 286–294, https://doi.org/10.1177/1947603513495889.
[52] H. Zhou, U.C. Ugbolue, Biomechanical analysis of lower limbs based on unstable condition sports footwear: a systematic review, Physical Activity and Health 8 (2024) 93–104, https://doi.org/10.5334/paah.332.
[53] C.M. Powers, The influence of abnormal hip mechanics on knee injury: a biomechanical perspective, J. Orthop. Sports Phys. Ther. 40 (2010) 42–51, https://doi.org/10.2519/jospt.2010.3337.
[54] M.D. LaPrade, M.I. Kennedy, C.A. Wijdicks, R.F. LaPrade, Anatomy and biomechanics of the medial side of the knee and their surgical implications, Sports Med. Arthrosc. Rev. 23 (2015) 63–70, https://doi.org/10.1097/JSA.0000000000000054.
[55] K. Kubo, D. Miyazaki, S. Tanaka, S. Shimoju, N. Tsunoda, Relationship between Achilles tendon properties and foot strike patterns in long-distance runners, J. Sports Sci. 33 (2015) 665–669, https://doi.org/10.1080/02640414.2014.962576.